Higher-order finite-element distributions in statistical theory of nuclear spectra

Maciej M. Duras* and Krzysztof Sokalski†
Institute of Physics, Jagellonian University, ulica Reymonta 4, 30-059 Krakow, Poland
(Received 26 December 1995; revised manuscript received 26 March 1996)

There are several standard methods that allow for the identification of a description of quantum chaotic systems. In this paper we discuss characteristics of quantum chaos, namely, the distributions of the following finite elements: asymmetrical three point first finite element of the three adjacent energy levels, the symmetrical three point first finite element of the three adjacent energy levels, and the second difference. The probability density functions of these three cases were calculated for the three-dimensional Gaussian orthogonal ensemble, Gaussian unitary ensemble, Gaussian symplectic ensemble, and for the quantum integrable three level system. We compare these distributions with the experimental data aiming at better classification of quantum systems (determining whether they are chaotic or integrable). A hypothesis is formulated: for both integrable and chaotic systems the energy levels have a tendency towards homogeneity. Finally we discuss the role of the discrete analogy to the curvature of levels. [S1063-651X(96)01109-9]

PACS number(s): 05.45.+b, 24.60.Lz, 24.60.Ky

I. INTRODUCTION

The basic tool allowing one to study quantum chaos in many level systems is nearest neighbor spacing, that is the difference between the adjacent levels. In an ascending sequence of energy levels of the many level quantum chaotic system one obtains a shortage of small spacings, observed in some nuclear and molecular spectra. To explain this phenomenon Wigner assumed the Gaussian orthogonal ensemble GOE(2); the Hamiltonian matrix elements were independent random variables (see [1–4]). This statistical hypothesis led to the proper description of level repulsion.

The ith spacing $s_i=E_{i+1}-E_i$ $(i=1,\ldots,n)$ is the simplest case of the finite element and it is not a proper tool to describe homogeneity of the energy distribution or long range correlation effects between levels as any of s_i is strictly local. Such information, however, can be extracted from the distributions of the higher-order finite elements. In order to obtain a better than standard [1–4] statistical description of the quantum level system we have derived analytic formulas for the distributions of some higher finite elements [5,6]. In [5] we studied the ith second difference $\Delta^2 E_i$ of the three adjacent energy levels E_i, E_{i+1}, E_{i+2}:

$$\Delta^2 E_i=\Delta^1 E_{i+1}-\Delta^1 E_i=E_i+E_{i+2}-2E_{i+1},\quad i=1,\ldots,n-1. \tag{1}$$

We demonstrated that the probability density function of the second difference has a universal character. The probability density function of the second difference was computed analytically for the following ensembles: GOE(3), Gaussian unitary ensemble [GUE(3)], Gaussian symplectic ensemble [GSE(3)], and for the quantum integrable three level system. In [6] we studied the three energy level quantum system and we derived the probability density functions of the three point finite elements of energy levels for the GOE(3), GUE(3), GSE(3), and for the quantum integrable system. We studied the following three point finite elements:

$$\Delta^1_{a,\mathrm{fin}}E_i=\frac{1}{2(i+1-i)}(-3E_i+4E_{i+1}-E_{i+2}) \tag{2}$$

(compare [7]; we named $\Delta^1_{a,\mathrm{fin}}E_i$ the ith asymmetrical three point first finite element; below we call it the asymmetrical element) and

$$\Delta^1_{s,\mathrm{fin}}E_{i+1}=\frac{1}{2(i+1-i)}(E_{i+2}-E_i) \tag{3}$$

(compare [7]; we called $\Delta^1_{s,\mathrm{fin}}E_{i+1}$ the ith symmetrical three point first finite element or just the symmetrical element). We derived analytically the probability density functions of these finite elements for GOE(3), GUE(3), and GSE(3) as well as for the sequence of the three adjacent randomly distributed energy levels. The distribution of the quantity named first order spacing (or the next nearest neighbor spacing) for the ordered sequence of the levels randomly distributed is given in [8], formula (3). The explicit formulas for distributions of first order spacing were derived in [9], formula (6) for the GOE(3) and in [10], formula (89) for the GUE(3). To the best of our knowledge, the distribution for the GSE(3) was derived for the first time in [6]. The distributions of the symmetrical element and of the first order spacing are consistent. The analytic formulas for the above distributions for the GOE(3) and for the integrable system are given in the Appendix. We do not present the formulas for the GUE(3) and GSE(3) since the full formulas are contained in [5,6].

As introduced above, statistical measures carry partial information about the system, extracted from the joint probability density functions of n eigenvalues of a random matrix $f^{\beta}_{E_1,\ldots,E_N}(e_1,\ldots,e_N)$ [9,11–15].

The n-level correlation function $R_{Nn\beta}$ was introduced by Dyson [16] for the circular unitary ensemble of dimension N. The n-level correlation function is the joint probability density function of finding n levels, regardless of their order,

*Electronic address: duras@izis.if.uj.edu.pl
†Electronic address: sokalski@izis.if.uj.edu.pl

and the values of the remaining $N-n$ levels are varied and are integrated out. It can also be defined for the GOE(N), GUE(N), and GSE(N) as follows:

$$R_{Nn\beta}(e_1,\ldots,e_n) = \frac{N!}{(N-n)!}\int_{-\infty}^{\infty}\cdots\int_{-\infty}^{\infty} de_{n+1}\cdots de_N f^{\beta}_{E_1,\ldots,E_N} \times(e_1,\ldots,e_N). \quad (4)$$

Choosing the proper statistical measure depends on what information one wants to extract from (4). In the literature, there are different statistical measures derived from (4).

Dyson defined the n-level correlation function $P_{n\beta}$ of the n levels $E_1,\ldots,E_n$ assuming the circular unitary ensemble of the dimension N, for $N\to\infty$:

$$P_{n\beta}(e_1,\ldots,e_n)=\lim_{N\to\infty}\left(\frac{\pi}{D\sqrt{2N}}\right)^n R_{Nn\beta}(e_1,\ldots,e_n), \quad (5)$$

where D is the mean level spacing. He derived the exact formula for P_{22} [16]. He also succeeded, using the quaternion algebra, to derive the exact formulas for $P_{n\beta}$, $n=1,2,\ldots$, where $\beta=1,2,4$ stands for the circular orthogonal ensemble, circular unitary ensemble, and circular symplectic ensemble, respectively [17]. Mehta derived the n-level cluster function $P_{n\beta}$ for the GOE, GUE, and GSE ensemble [11]. Dyson and Mehta [15] defined the Δ_3 statistics, that is the least-square deviation of the staircase function from the best straight line fitting it. The variance $\Sigma^2(\overline{n})$ of the number of levels n in the interval of the length $\overline{n}$ has also been studied [14]. Both the former and the latter constitute the measures of the ''local'' two-level fluctuations of the spectrum. Haq, Pandey, and Bohigas introduced a spectral-averaged Δ_3 measure [18], and found very good agreement between the two-level correlations in the nuclear data ensemble (NDE) and the two-level correlations predicted by GOE. In Ref. [19] they studied the three level and four level correlations. They introduced the skewness γ_1, which is the function of two level and three level correlation functions, and the excess γ_2, which is the function of two, three, and four level correlation functions. These two fluctuation measures calculated for GOE are in good agreement with NDE.

Let us answer why we choose to work with finite elements. First of all, they are natural extensions of spacing. All n-point finite elements ($n\geqslant 2$) equivalent to the first differential quotient describe the level repulsion caused by long range correlations (for large n). The n-point second differences ($n\geqslant 3$) describe the homogeneity of levels including long range correlations. Naturally one can introduce the n-point higher-order differences describing even more fine details of the level distributions. Thus the finite-element distributions allow one to extract in a systematic way much information about higher correlation effects. Moreover, we will show in this paper that these statistical measures are very easy to apply for a comparison between the experimental data and theory. The aim of this paper is to compare the theoretical results for the distributions of the asymmetrical element, symmetrical element, second difference, and spacing with the experimental data.

This paper is organized as follows. In Sec. II the distribution of the spacing is compared with the distributions of the asymmetrical element, symmetrical element, second difference for the GOE, and for the three level quantum integrable system. In Sec. III we discuss the obtained results and formulate a hypothesis.

II. THE COMPARISON OF THE THEORETICAL RESULTS WITH THE EXPERIMENTAL DATA

In this section we study the nuclear spectrum and the random-sequence spectrum. According to classification based on the finite-element distributions, one of them belongs to the quantum chaotic system and the remaining one to the quantum integrable system. For every spectrum we study the distribution of spacing, symmetrical element, asymmetrical element, and second difference. The way to compare the theoretical distributions for the GOE ensembles and for the quantum integrable system with the experimental data is to make the above four notions dimensionless. This can be achieved by dividing them by the mean value of the spacing for GOE(2), GOE(3), and for the quantum integrable system, respectively. For the given experimental spectrum we make these notions dimensionless by dividing them by the mean value of the spacing calculated for the spectrum. Hence, we compare the distribution of the given notion for the GOE ensembles, and for the quantum integrable system with the histogram of the notion given from the experimental spectrum. All the details concerning the theoretical approach are given in the Appendix.

We present the distributions of spacing, asymmetrical element, symmetrical element, and second difference for the GOE ensembles, and for the quantum integrable system, and the corresponding experimental histograms in (a), (b), (c), and (d) of Figs. 1 and 2 respectively, where Figs. 1 and 2 show the two above-mentioned spectra. To do this we applied formulas (A2), (A6), (A8), (A10), (A12), (A14), (A16), and (A18). The experimental data were unfolded using the the procedure described in [20].

The first spectrum corresponds to ^{167}Er [21]. The levels in the spectrum have the same J^{π}. Analysis of this spectrum based on the spacing distribution is presented in [14] [compare Figs. 1(a) and 2(a) therein], and the system is classified as chaotic. We study the spectrum using the distributions of finite elements. Looking at Fig. 1(a) one can see that the system is chaotic, since the level repulsion is observed. The same conclusion comes from Fig. 1(b), because the experimental histogram can be fitted by the GOE(3) distribution; the maxima of both curves are at $x=1$ and the tails of the curves are close to each other for $x\leqslant 0$ and $x\geqslant 2$. Furthermore we notice that the maxima are not as sharp as the maximum of the distribution of the dimensionless asymmetrical element for the quantum integrable system. The sharp maximum means that the first derivative of the distribution has discontinuity. For confirmation of the chaotic character of the system see Fig. 1(c). The histogram and the GOE(3) distribution of the dimensionless symmetrical element fit well together: they have maxima at $x=1$ and they have the same values at the maxima. Moreover, their tails are

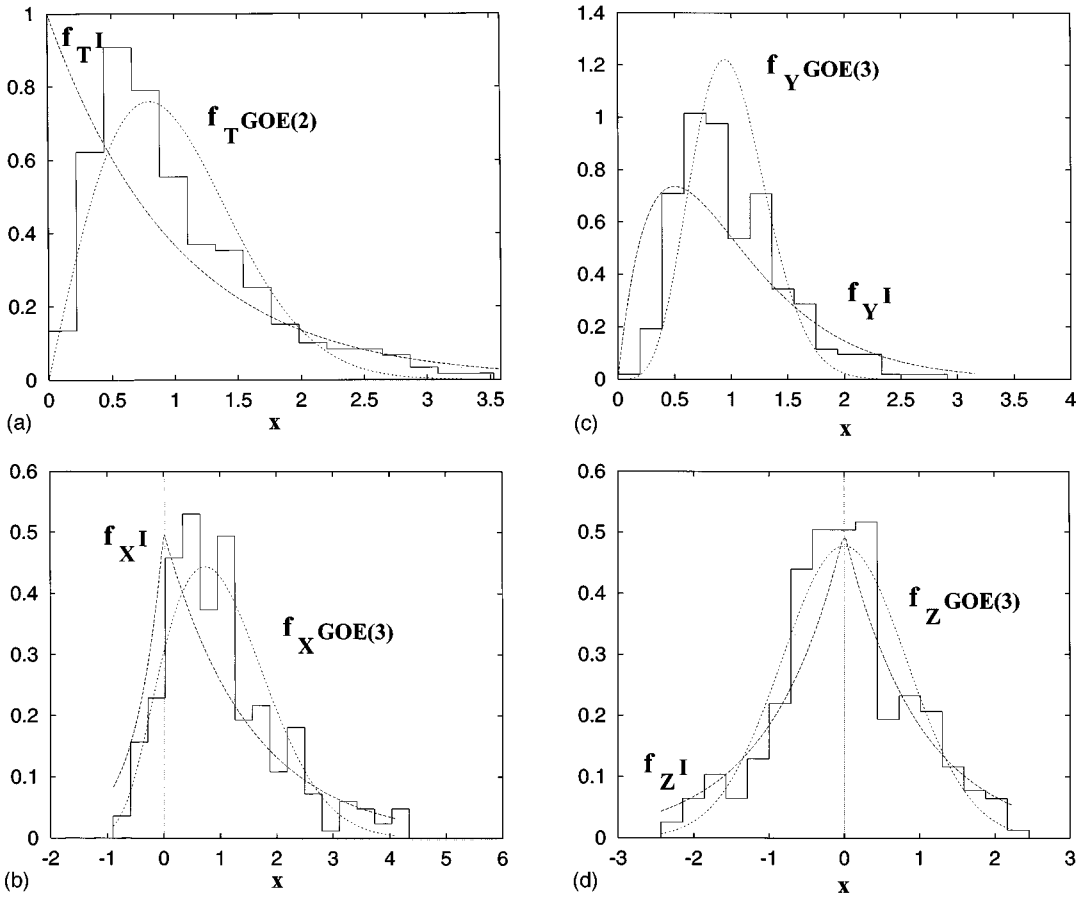

FIG. 1. (a) The probability density function of the dimensionless spacing for the GOE(2) (thin dashed line) for the integrable system (dashed line) and for ^{167}Er (histogram). (b) The probability density function of the dimensionless asymmetrical three point first finite element for the GOE(3) (thin dashed line), for the integrable system (dashed line) and for ^{167}Er (histogram). (c) The probability density function of the dimensionless symmetrical three point first finite element for the GOE(3) (thin dashed line) for the integrable system (dashed line) and for ^{167}Er (histogram). (d) The probability density function of the dimensionless second difference for the GOE(3) (thin dashed line), for the integrable system (dashed line), and for ^{167}Er (histogram).

close to each other for $0 \leqslant x \leqslant 0.5$ and for $x \geqslant 1.5$. The shortage of small values of the dimensionless symmetrical element is also observed, which is equivalent to the shortage of next nearest neighbor spacing. This means that the system is chaotic. The results from Fig. 1(d) also confirm that the system is chaotic, since the distribution of the dimensionless second difference for the GOE(3) and the histogram of the dimensionless second difference are in accordance with each other. Their maxima are at $x=0$, and the maxima are not sharp [compare the sharpness of the maximum of the distribution of the dimensionless second difference for the quantum integrable system; see Fig. 1(d)]. Moreover, their tails are close to each other for $x \leqslant -1$ and for $x \geqslant 1$. To make a short summary: the distributions of all the four notions point to chaos of the system.

The second spectrum corresponds to our numerical simulation of the random-sequence spectrum of length 2500. A similar simulation was made in [14] [compare Figs. 1(d) and 2(d) therein]. The system was classified as integrable. Looking at Fig. 2(a) one easily deduces that the system is integrable, because the small spacings are dominant and the histogram and the distribution of dimensionless spacing for the integrable case fit excellently. From Fig. 2(b) we recognize that the system is integrable. The experimental histogram fits almost perfectly the distribution of the dimensionless asymmetrical element for the quantum integrable system, the maxima of both curves are at $x=0$ and the tails of the curves are close to each other on the whole domain. The maximum of the histogram and the maximum of the distribution of the dimensionless asymmetrical element for the quantum integrable system are very sharp. From Fig. 2(c) we also learn that the system is integrable. The histogram excellently fits the distribution of the dimensionless symmetrical element for the quantum integrable system. They have maxima at $x=0.5$, and they have approximately the same values at the maxima. Moreover, their tails are close to each other on the whole domain. The presence of small values of the dimensionless symmetrical element is observed. Finally Fig. 2(d) demonstrates that the system is integrable, since the distribution of the dimensionless second difference for the quantum integrable system and the histogram of the dimensionless second difference are in accordance with each other. They fit each other excellently. Their maxima are at $x=0$, and the maxima are very sharp. Their tails are close to each other for all x. In summary, all four notions predict the integrability of the system.

The clear message coming out of all these exercises is that it is important to study together the different distributions in

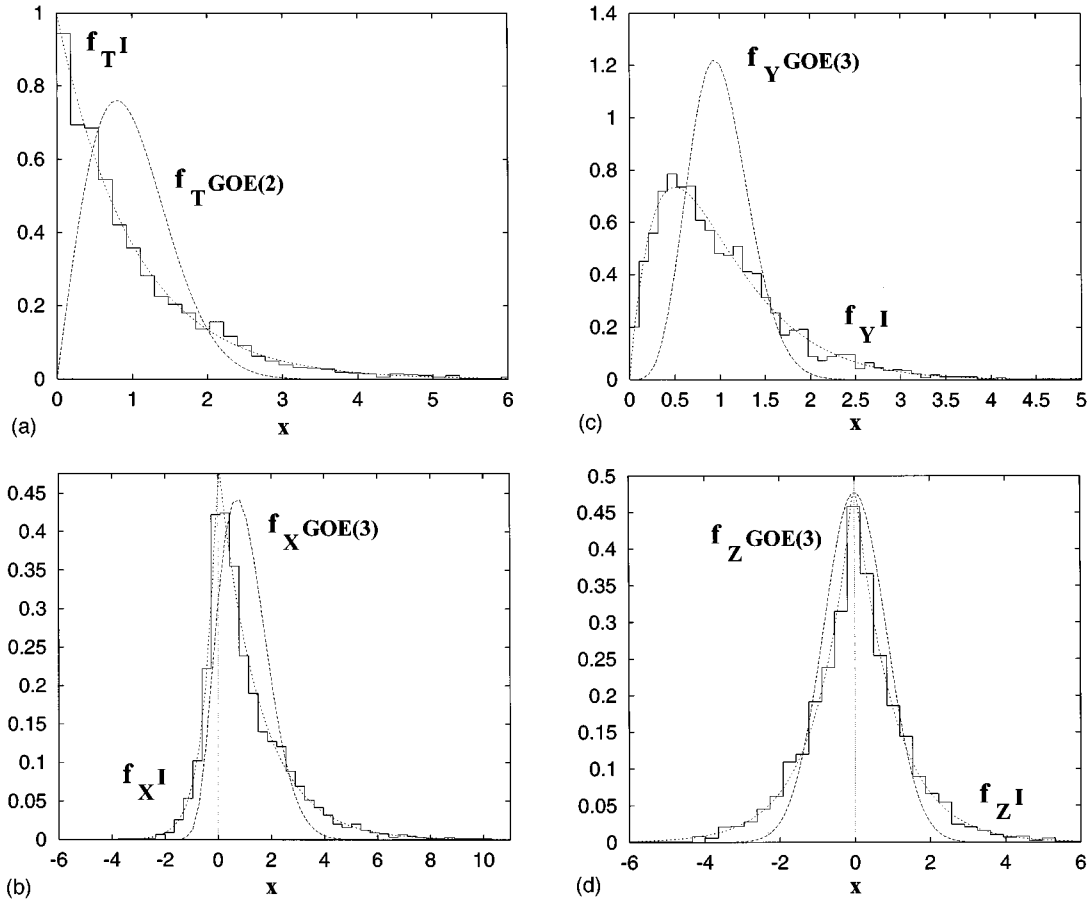

FIG. 2. (a) The probability density function of the dimensionless spacing for the GOE(2) (thin dashed line) for the integrable system (dashed line) and for random-sequence spectrum (histogram). (b) The probability density function of the dimensionless asymmetrical three point first finite element for the GOE(3) (thin dashed line), for the integrable system (dashed line), and for random-sequence spectrum (histogram). (c) The probability density function of the dimensionless symmetrical three point first finite element for the GOE(3) (thin dashed line), for the integrable system (dashed line), and for random-sequence spectrum (histogram). (d) The probability density function of the dimensionless second difference for the GOE(3) (thin dashed line), for the integrable system (dashed line), and for random-sequence spectrum (histogram).

order to classify the system. The confirmation of its chaos follows from the distributions of asymmetrical element, symmetrical element, and second difference.

The levels in the nuclear spectrum have the same values of J^{π}. The restriction of the spectrum to the subset of levels belonging to given J^{π} worsens significantly the statistics (the histogram resolution is poor). For this reason we are in great need of some additional quantity to help the classification of the system. Therefore, the asymmetrical element, symmetrical element, and second difference are quite helpful.

In order to classify a spectrum one should prepare the histograms of the dimensionless spacing, dimensionless asymmetrical element, dimensionless symmetrical element, and dimensionless second difference. Then, one must compare them with the respective theoretical distributions. We summarize the criteria of the comparisons of the distributions with the histograms. For the dimensionless spacing the absence of small spacing should be studied. For the dimensionless asymmetrical element the horizontal position of the maximum of the distributions and of the histogram must be compared, as well as the closeness of the tails and the presence of the sharpness of the maxima. For the dimensionless symmetrical element one should compare the horizontal and the vertical positions of the maxima, and the closeness of the tails. Finally, for the dimensionless second difference one must measure the closeness of the tails and the sharpness of the maxima.

We studied also the following 20 nuclear spectra from [22–41] corresponding to ^{181}Ta, ^{143}Nd, ^{156}Gd, ^{160}Dy, ^{161}Dy, ^{162}Dy, ^{163}Dy, ^{164}Dy, ^{166}Er, ^{167}Er, ^{168}Er p wave resonance, ^{168}Er s wave resonance, ^{170}Er p wave resonance, ^{170}Er s wave resonance, ^{164}Er, ^{45}Sc, $J^{\pi}=\frac{1}{2}^{+}$ states, ^{45}Sc, $J^{\pi}=\frac{1}{2}^{-}$ states, ^{45}Sc, $l=2$ states, ^{45}Sc, $J^{\pi}=\frac{3}{2}^{-}$ states, ^{49}V, respectively and one molecular spectrum from [42] corresponding to NO_2 [43]. All the above-mentioned 21 spectra are in accordance with the theory.

III. CONCLUSIONS

We presented statistical measures: the distribution of the second difference, the asymmetrical element, and the symmetrical element. They supplement the distribution of spacing as good tools for the classification of the quantum system. The distributions of all the investigated tools and of the spacing agree; i.e., all of them assign the system to the same class. The decision on the classification of the system now

depends on the conjunction of four expressions related to the above four distributions. All the derived distributions of the second difference have their maxima at the origin. This means a tendency of the systems towards the homogeneous distribution of the levels. All the collected experimental data are consistent with this formulation. On the basis of our theoretical results (A10), (A18), as well as on the basis of the experimental data [Figs. 1(d) and 2(d)] we stated the following hypothesis: For both integrable and chaotic systems, energy levels show a certain homogeneity of distribution.

The differences between the probability density functions of the second difference for the chaotic and integrable cases are described in detail. The detection of that detail demands good resolution model computations with very good level statistics.

The ith energy level E_i might be treated as a value of the discrete function f of its *discrete* index i, namely,

$$f: I \ni i \to E_i \in E, \tag{6}$$

where I is the discrete energy index set and E is the discrete energy value set, and $f(i)=E_i$. The function f is monotonic, because the levels are ordered and undegenerated. We assume that f is monotonic increasing since energy levels E_i are ordered increasingly: $...\leqslant E_{i-1}\leqslant E_i\leqslant E_i\leqslant ...$. Hence the ith spacing s_i is the first difference between the two adjacent energies E_i, E_{i+1} and it is also the first differential quotient of the function f at the point i. The ith second difference $\Delta^2 E_i$ is the second difference of the three adjacent energies E_i, E_{i+1}, E_{i+2} and it is also the second differential quotient of the function f at the point i:

$$\Delta^2 E_i = \frac{\Delta^2 f(i)}{\Delta i^2}. \tag{7}$$

We can treat the discrete set I of all the indexes i of the energy levels E_i as an abstract space. Hence the second difference (1) might be seen as the curvature of the energy function f with respect to the discrete argument i in the product space $I\times E$.

The above interpretation of the second differential quotient should be compared to the curvature of energy levels introduced by Zakrzewski and Delande and Zakrzewski, Delande, and Kuś [44,45]. The ''motion'' of the levels with respect to the ''fictitious'' time λ is studied. Namely, the Hamiltonian operator of the quantum system H linearly depends on the *continuous* parameter λ:

$$H(\lambda) = H_1 + \lambda H_2, \tag{8}$$

where H_1 and H_2 are the operators describing some parts of the dynamics. Hence, the second derivative of the energy level with respect to λ is introduced:

$$K = \frac{d^2 E(i)}{d\lambda^2} = \frac{d^2 f(i)}{d\lambda^2}. \tag{9}$$

The second derivative K is called the ''curvature'' of levels. Comparing (7) with (9) one easily sees that the second difference is the discrete analogy of the continuous curvature in ''perpendicular'' direction to λ. Hence, we can treat the second difference as the curvature of the level E_i with respect to its discrete label parameter i. We point out some differences in both approaches. The change of the parameter λ causes the change of the system, but the change of the parameter i causes the change of the energy in the same system. This means that the study of the distribution of the curvature with respect to the parameter λ is a tool for comparing these different yet similar systems [small changes of λ cause small changes of Hamiltonian $H(A)$], whereas the study of the system by the distribution of the second difference allows one to investigate one system without perturbation. This approach introduces other information about the system than K. Therefore two approaches, the use of the distribution of second difference $\Delta^2 E_i$ and of the distribution of curvature K, are not equivalent to each other. Combination of these methods together makes the investigation space ''two dimensional'': one can study the changes of the function f with respect to i and to λ (''space'' and ''time'' coordinates).

APPENDIX

We assume the GOE(2). The mean spacing for the GOE(2) reads [compare [46], formula (6.6.10)]

$$\overline{S^{\mathrm{GOE}(2)}} = \sqrt{2\pi}\sigma, \tag{A1}$$

where σ^2 is the variance of the off-diagonal elements of the GOE(2) matrix. We can make the spacing dimensionless by dividing it by the mean spacing $\overline{S^{\mathrm{GOE}(2)}}$. We define the new dimensionless spacing for the GOE(2) as

$$T^{\mathrm{GOE}(2)} = s_1 / \overline{S^{\mathrm{GOE}(2)}}. \tag{A2}$$

The probability density function of $T^{\mathrm{GOE}(2)}$ is [46] formula (6.6.11):

$$f_{T^{\mathrm{GOE}(2)}}(x) = \Theta(x)\frac{\pi}{2}x\exp\left(-\frac{\pi x^2}{4}\right), \tag{A3}$$

where Θ is the Heaviside function:

$$\Theta(x) = \begin{cases} 1 & \text{for } x \geqslant 0 \\ 0 & \text{for } x < 0. \end{cases}$$

Now, we assume the GOE(3). The mean spacing for the GOE(3) reads [compare [9], formula (5)]

$$\overline{S^{\mathrm{GOE}(3)}} = \frac{3\sqrt{3}\sigma}{\sqrt{2\pi}}, \tag{A4}$$

where σ^2 is the variance of the off-diagonal elements of the GOE(3) matrix. The asymmetrical element is made dimensionless by dividing it by the mean spacing $\overline{S^{\mathrm{GOE}(3)}}$. We define the new dimensionless random variable for the GOE(3) as

$$X^{\mathrm{GOE}(3)} = \Delta^1_{a,\mathrm{fin}} E_1 / \overline{S^{\mathrm{GOE}(3)}}. \tag{A5}$$

The probability density function of $X^{\mathrm{GOE}(3)}$ reads [6]

$$f_{X^{\mathrm{GOE}(3)}}(x)=\frac{81}{228488\pi^2}\left[910\sqrt{13}\pi x-315\sqrt{13}x^3+(1638x^2+2704\pi)\exp\left(-\frac{25x^2}{52\pi}\right)+\sqrt{13}x(315x^2-910\pi)\mathrm{erf}\left(\frac{5x}{2\sqrt{13\pi}}\right)\right]\times\exp\left(-\frac{27x^2}{52\pi}\right)\quad\text{for } x\geqslant 0,$$

$$f_{X^{\mathrm{GOE}(3)}}(x)=-\frac{81}{228488\pi^2}\left[-910\sqrt{13}\pi x+315\sqrt{13}x^3+(390x^2-2704\pi)\exp\left(-\frac{441x^2}{52\pi}\right)+\sqrt{13}x(315x^2-910\pi)\mathrm{erf}\left(\frac{21x}{2\sqrt{13\pi}}\right)\right]\times\exp\left(-\frac{27x^2}{52\pi}\right)\quad\text{for } x<0, \tag{A6}$$

where the error function is

$$\mathrm{erf}(x)=\frac{2}{\sqrt{\pi}}\int_0^x dt\,\exp(-t^2).$$

The symmetrical element is made dimensionless by defining the following dimensionless random variable for the GOE(3):

$$Y^{\mathrm{GOE}(3)}=\Delta^1_{s,\mathrm{fin}}E_1/\overline{S^{\mathrm{GOE}(3)}}. \tag{A7}$$

The probability density function of $Y^{\mathrm{GOE}(3)}$ is [6]

$$f_{Y^{\mathrm{GOE}(3)}}(x)=\frac{81x}{4\pi^2}\left[6x\exp\left(-\frac{9x^2}{\pi}\right)+(9x^2-2\pi)\times\exp\left(-\frac{27x^2}{4\pi}\right)\mathrm{erf}\left(\frac{3x}{2\sqrt{\pi}}\right)\right]. \tag{A8}$$

In order to make the second difference dimensionless we divide it by the mean spacing $\overline{S^{\mathrm{GOE}(3)}}$ and we define the new dimensionless random variable for the GOE(3)

$$Z^{\mathrm{GOE}(3)}=\Delta^2E_1/\overline{S^{\mathrm{GOE}(3)}}. \tag{A9}$$

The probability density function of $Z^{\mathrm{GOE}(3)}$ reads [5]

$$f_{Z^{\mathrm{GOE}(3)}}(x)=\frac{3}{2\pi}\exp\left(-\frac{9x^2}{4\pi}\right). \tag{A10}$$

We assume now the quantum integrable system. The mean spacing throughout the level sequence is equal to D [8]. We make the spacing dimensionless by dividing it by the mean spacing D. We define the new dimensionless spacing for the quantum integrable system:

$$T^I=s_1/D. \tag{A11}$$

The probability density function of T^I is [compare [8], formula (3)]

$$f_{T^I}(x)=\Theta(x)\exp(-x). \tag{A12}$$

We make the asymmetrical element dimensionless by dividing it by the mean spacing D. We define the new dimensionless random variable for the quantum integrable system:

$$X^I=\Delta^1_{a,\mathrm{fin}}E_1/D. \tag{A13}$$

The probability density function of X^I is [6]

$$f_{X^I}(x)=\begin{cases}\frac{1}{2}\exp(-2x/3) & \text{for } x\geqslant 0\\ \frac{1}{2}\exp(2x) & \text{for } x<0.\end{cases} \tag{A14}$$

We make the symmetrical element dimensionless by defining the following dimensionless random variable for the quantum integrable system:

$$Y^I=\Delta^1_{s,\mathrm{fin}}E_1/D. \tag{A15}$$

The probability density function of Y^I reads [6]

$$f_{Y^I}(x)=\Theta(x)4x\exp(-2x). \tag{A16}$$

In order to make the second difference dimensionless we divide it by the mean spacing D and we define the new dimensionless random variable for the quantum integrable system

$$Z^I=\Delta^2E_1/D. \tag{A17}$$

The probability density function of Z^I is [5]

$$f_{Z^I}(x)=\tfrac{1}{2}\exp(-|x|). \tag{A18}$$

[1] E.P. Wigner, International Conference on the Neutron Interactions with the Nucleus, Columbia University, New York, 1957, Columbia University Report No. CU-175 (TID-7547), 1957, p. 49.

[2] E.P. Wigner, Conference on Neutron Physics by Time-of-Flight, Gatlinburg, Tennessee, 1956, Oak Ridge National Laboratory Report No. ORNL-2309, 1957, p. 59.

[3] C.E. Porter, *Statistical Theories of Spectra: Fluctuations* (Academic, New York, 1965), p. 223.

[4] *Statistical Theories of Spectra: Fluctuations* (Ref. [3]), p. 199.

[5] M. M. Duras and K. Sokalski, Phys. Rev. E (to be published).

[6] M. M. Duras and K. Sokalski, Phys. Rev. E (to be published).

[7] L. Collatz, *Numerische Behandlung von Differentialgleichungen* (Springer-Verlag, Berlin, 1955), Appendix, Table II.

[8] C.E. Porter, *Statistical Theories of Spectra: Fluctuations* (Ref. [3]), p. 6.
[9] C.E. Porter, Nucl. Phys. **40**, 167 (1963).
[10] P.B. Kahn and C.E. Porter, Nucl. Phys. **48**, 385 (1963).
[11] M.L. Mehta, Commun. Math. Phys. **20**, 245 (1971).
[12] C.E. Porter, *Statistical Theories of Spectra: Fluctuations* (Ref. [3]), p. 3.
[13] M.L. Mehta, *Random Matrices and the Statistical Theory of Energy Levels* (Academic, New York, 1967).
[14] T.A. Brody, J. Flores, J.B. French, P.A. Mello, A. Pandey, and S.S.M. Wong, Rev. Mod. Phys. **53**, 385 (1981).
[15] F.J. Dyson and M.L. Mehta, J. Math. Phys. **4**, 701 (1963).
[16] F.J. Dyson, J. Math. Phys. **3**, 166 (1962).
[17] F.J. Dyson, Commun. Math. Phys. **19**, 235 (1970).
[18] R.U. Haq, A. Pandey, and O. Bohigas, Phys. Rev. Lett. **48**, 1086 (1982).
[19] O. Bohigas, R.U. Haq, and A. Pandey, Phys. Rev. Lett. **54**, 1645 (1985).
[20] E. Haller, H. Köppel, and L.S. Cederbaum, Chem. Phys. Lett. **101**, 215 (1983).
[21] H.I. Liou, H.S. Camarda, S. Wynchank, M. Slagowitz, G. Hacken, F. Rahn, and J. Rainwater, Phys. Rev. C **5**, 974 (1972), Table III.
[22] G. Hacken, R. Werbin, and J. Rainwater, Phys. Rev. C **17**, 43 (1978), Table I.
[23] J. Wrzesiński, A. Clauberg, C. Wesselborg, R. Reinhardt, A. Dewald, K.O. Zell, P. von Brentano, and R. Broda, Nucl. Phys. **A515**, 297 (1990), Table I.
[24] C. Coceva and M. Stefanon, Nucl. Phys. **A315**, 1 (1979), Table I.
[25] H.I. Liou, G. Hacken, J. Rainwater, and U.N. Singh, Phys. Rev. C **11**, 462 (1975), Table I.
[26] Liou *et al.* (Ref. [25]), Table II.
[27] Liou *et al.* (Ref. [25]), Table III.
[28] Liou *et al.* (Ref. [25]), Table IV.
[29] Liou *et al.* (Ref. [25]), Table V.
[30] H.I. Liou, H.S. Camarda, S. Wynchank, M. Slagowitz, G. Hacken, F. Rahn, and J. Rainwater, Phys. Rev. C **5**, 974 (1972), Table II.
[31] Liou *et al.* (Ref. [30]), Table X.
[32] Liou *et al.* (Ref. [30]), Table V, *p* wave resonance.
[33] Liou *et al.* (Ref. [30]), Table IV, *s* wave resonance.
[34] Liou *et al.* (Ref. [30]), Table VII, *p* wave resonance.
[35] Liou *et al.* (Ref. [30]), Table VI, *s* wave resonance.
[36] Liou *et al.* (Ref. [30]), Table VIII.
[37] W.M. Wilson, E.G. Bilpuch, and G.E. Mitchell, Nucl. Phys. **A245**, 262 (1975), Table I, $J^\pi = \frac{1}{2}^+$ states.
[38] Wilson, Bilpuch, and Mitchell (Ref. [37]), Table I, $J^\pi = \frac{1}{2}^-$ states.
[39] Wilson, Bilpuch, and Mitchell (Ref. [37]), Table I, $l = 2$ states.
[40] Wilson, Bilpuch, and Mitchell (Ref. [37]), Table I, $J^\pi = \frac{3}{2}^-$ states.
[41] N.H. Prochnow, H.W. Newson, E.G. Bilpuch, and G.E. Mitchell, Nucl. Phys. **A194**, 353 (1972), Table II.
[42] R.E. Smalley, L. Wharton, and D.H. Levy, J. Chem. Phys. **63**, 4977 (1975), Table I.
[43] M. M. Duras, Ph.D. thesis, Jagellonian University, Cracow, 1996.
[44] J. Zakrzewski and D. Delande, Phys. Rev. E **47**, 1650 (1993).
[45] J. Zakrzewski, D. Delande, and M. Kuś, Phys. Rev. E **47**, 1665 (1993).
[46] L.E. Reichl, *The Transition to Chaos In Conservative Classical Systems: Quantum Manifestations* (Springer-Verlag, New York, 1992), Chap. 6, p. 248.